Model Stability from Shell far

Frédéric Nowacki[1]

International Collaborations in nuclear theory:
Theory for open-shell nuclei near the limits of stability

[1]Strasbourg-Madrid Shell-Model collaboration

Landscape of medium mass nuclei

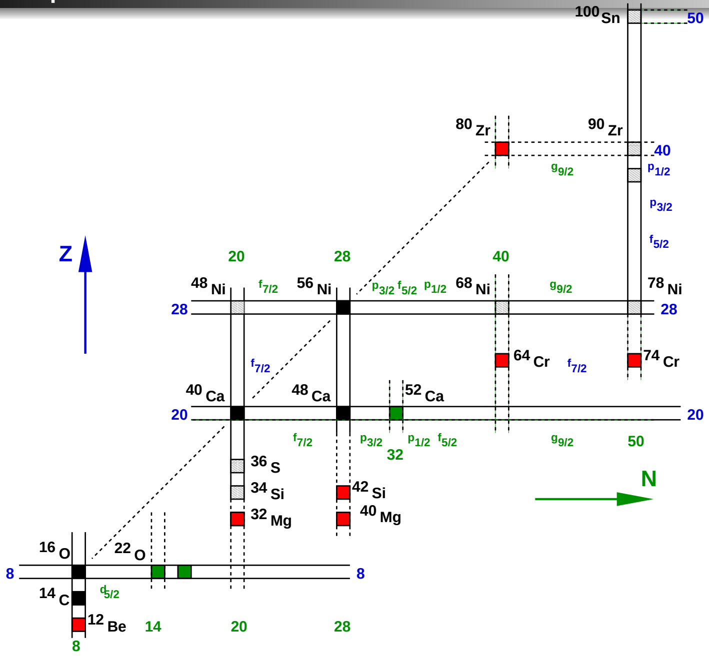

Landscape of medium mass nuclei

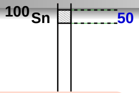

UNDERSTANDING REGULARITIES
for both SPHERICAL and DEFORMED systems

- Magic Numbers: ^{24}O, ^{48}Ni, ^{54}Ca, ^{78}Ni, ^{100}Sn
- Islands of Deformation: ^{12}Be, ^{32}Mg, ^{42}Si, ^{64}Cr, ^{80}Zr ...

- Variety of phenomena dictated by shell structure
- Close connection between collective behaviour and underlying shell structure
- $$\mathcal{H} = \mathcal{H}_m + \mathcal{H}_{\mathcal{M}}$$

Interplay between
- Monopole field (spherical mean field)
- Multipole correlations (pairing, Q.Q, ...)

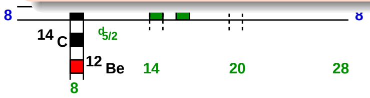

Effective Single Particle Energies: Trends

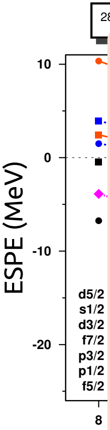

- Magic numbers are associated to enegy gaps in the spherical mean field. Therefore, to promote particles above the Fermi levels costs energy
- However some intruders configurations can overwhelm their loss of monopole energy with their huge gain in correlation energy
- Several examples of this phenomenon exist in stable magic nuclei (as in ^{40}Ca nucleus) in the form of coexisting spherical, deformed and superdeformed states in a very narrow energy range
- At the very neutron rich or very proton rich edges, the T=0 and T=1 channels of the effective nuclear interaction weight very differently than they do at the stability line. Therefore the effective single particle structure may suffer important changes, leading in some cases to the vanishing of established shell closures or to the appearance of new ones

Effective Single Particle Energies: Trends

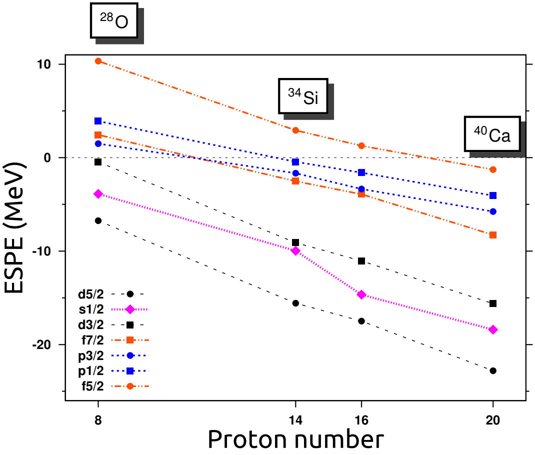

- At the neutron drip line, the ESPE's of ^{28}O are completely at variance with those of ^{40}Ca at the stability valley. The change from the standard ESPE's of ^{16}O to the anomalous ones in ^{28}O is totally due to the interactions of *sd* shell neutrons among themselves
- Notice that the *sd* shell orbits remain always below th *pf* shell with the $\nu 0f_{\frac{7}{2}}$ and $\nu 0p_{\frac{3}{2}}$ orbitals DO get inverted
- The monopole part of the neutron-proton interaction restores the N=20 shell gap when the valley of stability is approached
- Spin-Tensor decomposition shows it is mainly a Central and Tensor effect

Effective Single Particle Energies: Trends

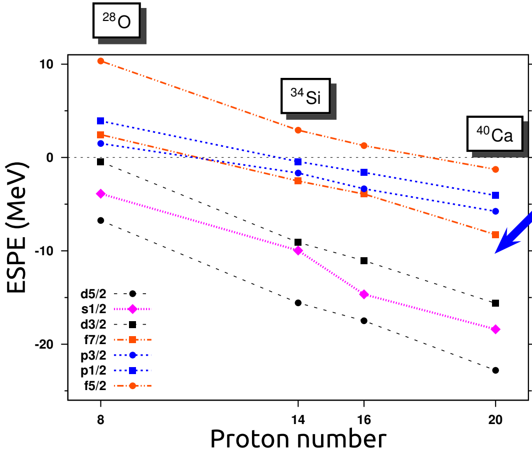

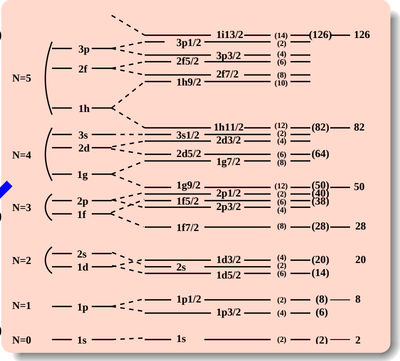

- N=20 shell gap when the valley of stability is approached
- Spin-Tensor decomposition shows it is mainly a Central and Tensor effect

Effective Single Particle Energies: Trends

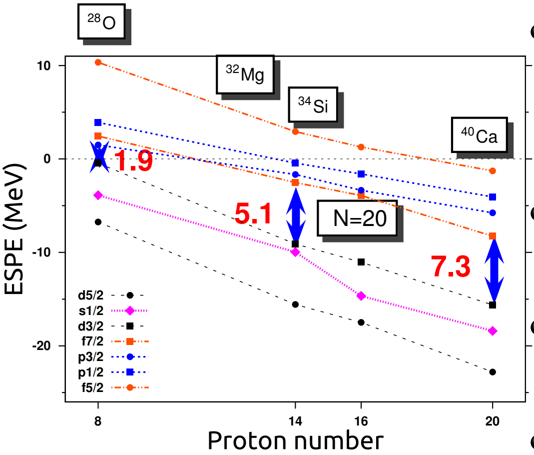

- At the neutron drip line, the ESPE's of ^{28}O are completely at variance with those of ^{40}Ca at the stability valley. The change from the standard ESPE's of ^{16}O to the anomalous ones in ^{28}O is totally due to the interactions of *sd* shell neutrons among themselves
- Notice that the *sd* shell orbits remain always below th *pf* shell with the $\nu 0f_{\frac{7}{2}}$ and $\nu 0p_{\frac{3}{2}}$ orbitals DO get inverted
- The monopole part of the neutron-proton interaction restores the N=20 shell gap when the valley of stability is approached
- Spin-Tensor decomposition shows it is mainly a Central and Tensor effect

Effective Single Particle Energies: Trends

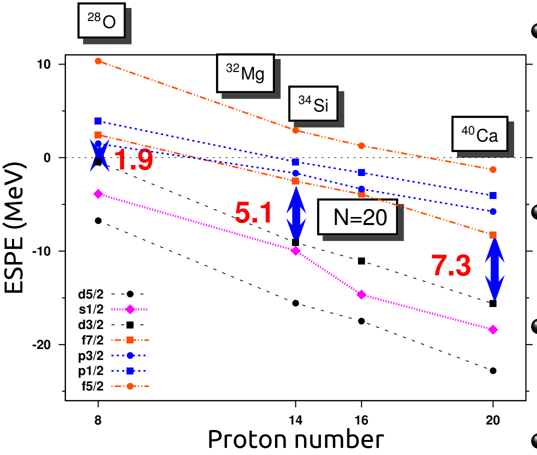

- At the neutron drip line, the ESPE's of ^{28}O are completely at variance with those of ^{40}Ca at the stability valley. The change from the standard ESPE's of ^{16}O to the anomalous ones in ^{28}O is totally due to the interactions of *sd* shell neutrons among themselves
- Notice that the *sd* shell orbits remain always below th *pf* shell with the $\nu 0f_{\frac{7}{2}}$ and $\nu 0p_{\frac{3}{2}}$ orbitals DO get inverted
- The monopole part of the neutron-proton interaction restores the N=20 shell gap when the valley of stability is approached
- Spin-Tensor decomposition shows it is mainly a Central and Tensor effect

Effective Single Particle Energies: Trends

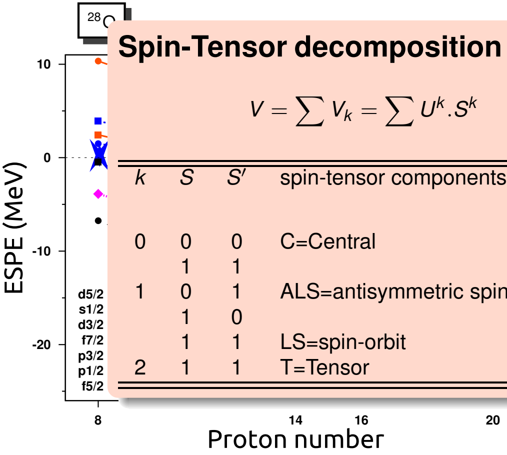

Spin-Tensor decomposition

$$V = \sum V_k = \sum U^k . S^k$$

k	S	S'	spin-tensor components
0	0	0	C=Central
	1	1	
1	0	1	ALS=antisymmetric spin-orbit
	1	0	
	1	1	LS=spin-orbit
2	1	1	T=Tensor

eutron drip line, the ESPE's of completely at variance with ^{40}Ca at the stability valley. The rom the standard ESPE's of e anomalous ones in ^{28}O is e to the interactions of *sd* shell among themselves

at the *sd* shell orbits remain elow th *pf* shell with the $\nu 0f_{\frac{7}{2}}$ $_{\frac{3}{2}}$ orbitals DO get inverted

opole part of the roton interaction restores the ell gap when the valley of s approached

- Spin-Tensor decomposition shows it is mainly a Central and Tensor effect

Effective Single Particle Energies: Trends

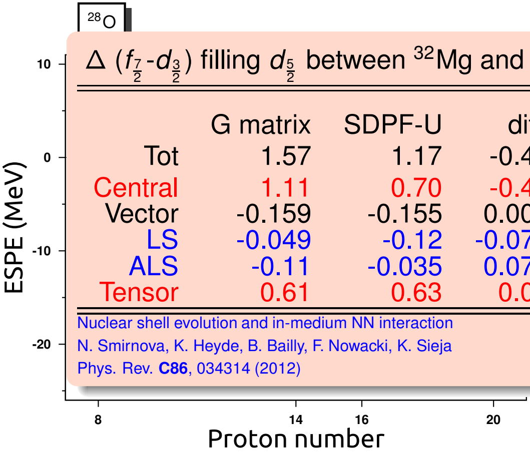

Δ ($f_{\frac{7}{2}}$-$d_{\frac{3}{2}}$) filling $d_{\frac{5}{2}}$ between ^{32}Mg and ^{34}Si

	G matrix	SDPF-U	diff.
Tot	1.57	1.17	-0.40
Central	1.11	0.70	-0.41
Vector	-0.159	-0.155	0.004
LS	-0.049	-0.12	-0.071
ALS	-0.11	-0.035	0.075
Tensor	0.61	0.63	0.02

Nuclear shell evolution and in-medium NN interaction
N. Smirnova, K. Heyde, B. Bailly, F. Nowacki, K. Sieja
Phys. Rev. **C86**, 034314 (2012)

- ...n drip line, the ESPE's of ...etely at variance with ...at the stability valley. The ...he standard ESPE's of ...malous ones in ^{28}O is ...he interactions of *sd* shell ...ng themselves

  ... *sd* shell orbits remain ...th *pf* shell with the $\nu 0f_{\frac{7}{2}}$ ...itals DO get inverted

  ... part of the ...n interaction restores the ...o when the valley of ...roached

- Spin-Tensor decomposition shows it is mainly a Central and Tensor effect

Effective Single Particle Energies: Trends

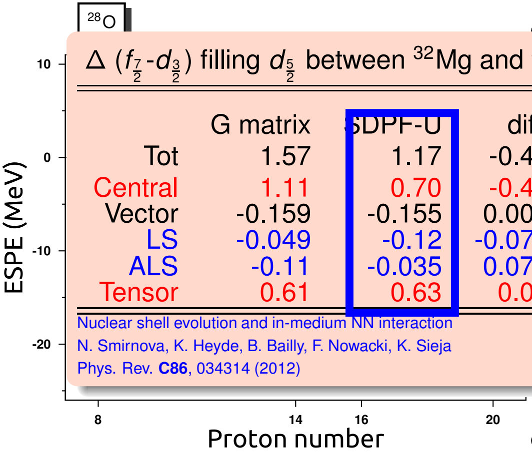

Δ ($f_{\frac{7}{2}}$-$d_{\frac{3}{2}}$) filling $d_{\frac{5}{2}}$ between ^{32}Mg and ^{34}Si

	G matrix	SDPF-U	diff.
Tot	1.57	1.17	-0.40
Central	1.11	0.70	-0.41
Vector	-0.159	-0.155	0.004
LS	-0.049	-0.12	-0.071
ALS	-0.11	-0.035	0.075
Tensor	0.61	0.63	0.02

Nuclear shell evolution and in-medium NN interaction
N. Smirnova, K. Heyde, B. Bailly, F. Nowacki, K. Sieja
Phys. Rev. **C86**, 034314 (2012)

- At the neutron drip line, the ESPE's of ... etely at variance with ... at the stability valley. The ... ne standard ESPE's of ... malous ones in ^{28}O is ... he interactions of *sd* shell ... ng themselves
- ... *sd* shell orbits remain ... th *pf* shell with the $\nu 0f_{\frac{7}{2}}$ ... itals DO get inverted
- ... part of the ... interaction restores the ... o when the valley of ... roached
- Spin-Tensor decomposition shows it is mainly a Central and Tensor effect

Effective Single Particle Energies: Trends

1d3/
2s1/
1d5/

Δ (

C
T

PHYSICAL REVIEW C **79**, 034318 (2009)

Nuclear "bubble" structure in ^{34}Si

M. Grasso,[1] L. Gaudefroy,[2] E. Khan,[1] T. Nikšić,[3] J. Piekarewicz,[4] O. Sorlin,[5] N. Van Giai,[1] and D. Vretenar[3]

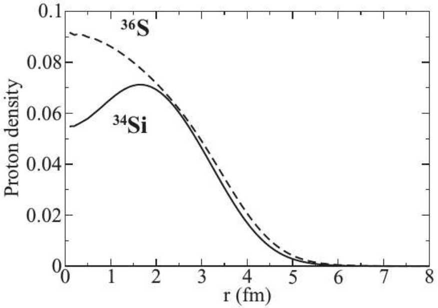

FIG. 4. HF charge densities (in units of fm^{-3}) of ^{36}S (dashed line) and ^{34}Si (solid line) calculated with the Skyrme interaction SLy4.

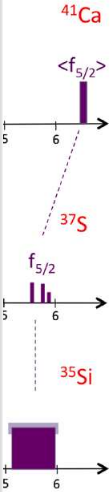

Effective Single Particle Energies: Trends

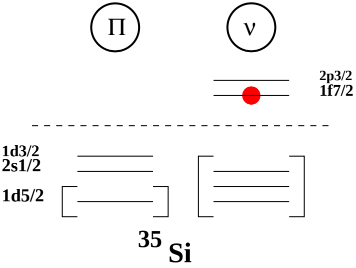

Δ ($p_{\frac{3}{2}}$-$p_{\frac{1}{2}}$) filling $s_{\frac{1}{2}}$ between ^{34}Si and ^{36}S

	KLS	N3LO (bare)	N3LO ($4\hbar\omega$)
Tot	0.58	0.58	0.60
Central	0.00	0.00	0.00
Vector	0.58	0.58	0.60
Tensor	0.00	0.00	0.00

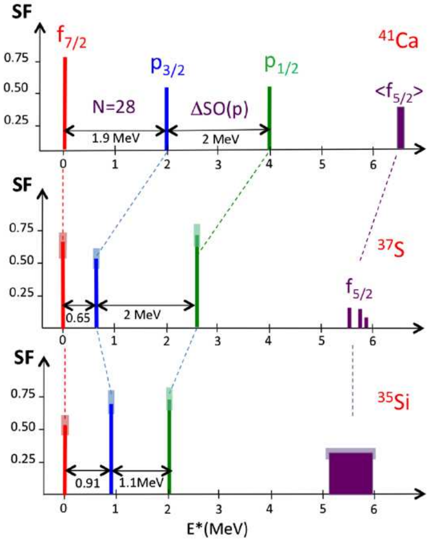

G. Burgunder, PhD Thesis GANIL, December 2011

Effective Single Particle Energies: Trends

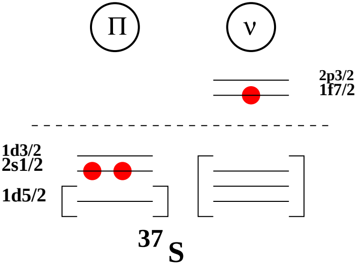

$\Delta\,(p_{\frac{3}{2}}\text{-}p_{\frac{1}{2}})$ filling $s_{\frac{1}{2}}$ between ^{34}Si and ^{36}S

	KLS	N3LO (bare)	N3LO ($4\hbar\omega$)
Tot	0.58	0.58	0.60
Central	0.00	0.00	0.00
Vector	0.58	0.58	0.60
Tensor	0.00	0.00	0.00

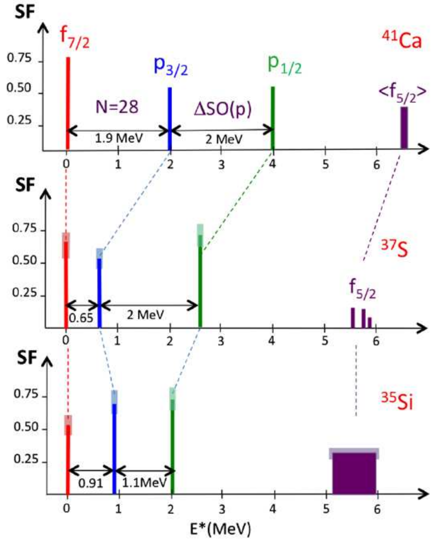

G. Burgunder, PhD Thesis GANIL, December 2011

Effective Single Particle Energies: Trends

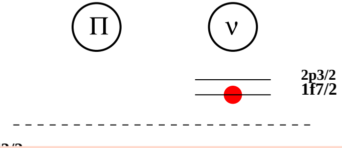

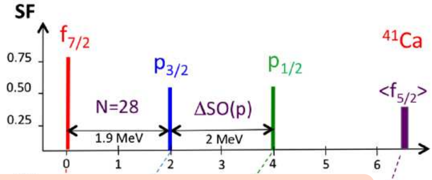

PRL 112, 042502 (2014) PHYSICAL REVIEW LETTERS week ending 31 JANUARY 2014

Experimental Study of the Two-Body Spin-Orbit Force in Nuclei

G. Burgunder,[1] O. Sorlin,[1] F. Nowacki,[2] S. Giron,[3] F. Hammache,[3] M. Moukaddam,[2] N. de Séréville,[3] D. Beaumel,[3] L. Càceres,[1] E. Clément,[1] G. Duchêne,[2] J. P. Ebran,[4] B. Fernandez-Dominguez,[1,5] F. Flavigny,[6] S. Franchoo,[3] J. Gibelin,[7] A. Gillibert,[6] S. Grévy,[1,8] J. Guillot,[3] A. Lepailleur,[1] I. Matea,[3] A. Matta,[3,9] L. Nalpas,[6] A. Obertelli,[6] T. Otsuka,[10] J. Pancin,[1] A. Poves,[11] R. Raabe,[1,12] J. A. Scarpaci,[13] I. Stefan,[3] C. Stodel,[1] T. Suzuki,[14] and J. C. Thomas[1]

		(bare)	($4\hbar\omega$)
Tot	0.58	0.58	0.60
Central	0.00	0.00	0.00
Vector	0.58	0.58	0.60
Tensor	0.00	0.00	0.00

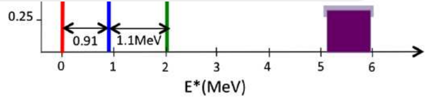

G. Burgunder, PhD Thesis GANIL, December 2011

Correlation Energies

- Let us consider the configurations with closed N=20 $[sd]^{12,Z}$ (normal filling) and the ones with two neutrons blocked in the *pf* shell $[sd]^{10,Z}[pf]^{2,0}$ (intruder)

- And calculate the energy of the ground states at fixed configuration, with and without correlations

Correlations energies: normal vs 2p-2h intruder

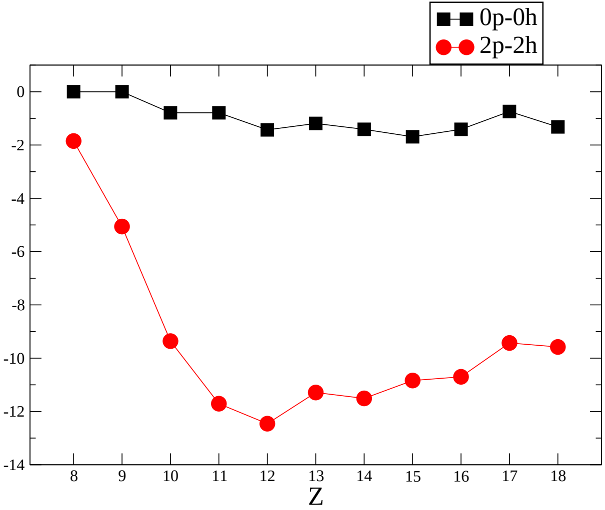

F. Nowacki and A. Poves
Phys. Rev. **C90**, 014302 (2014)

Correlations energies: normal vs 2p-2h intruder

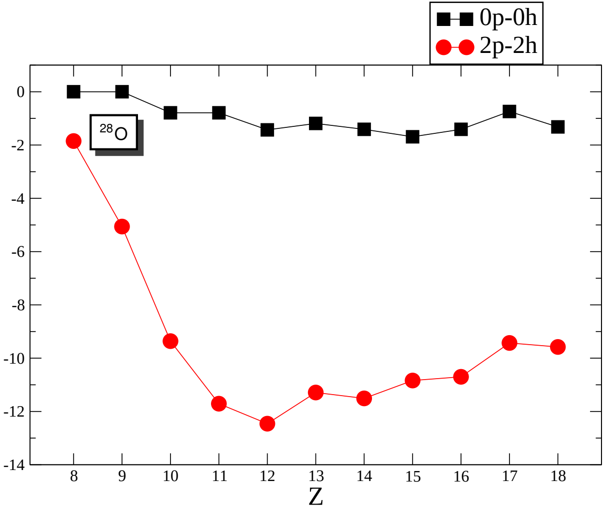

F. Nowacki and A. Poves
Phys. Rev. **C90**, 014302 (2014)

Correlations energies: normal vs 2p-2h intruder

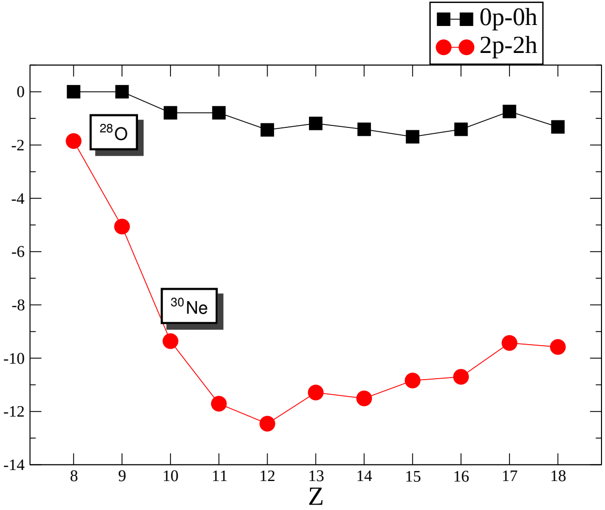

F. Nowacki and A. Poves
Phys. Rev. **C90**, 014302 (2014)

Correlations energies: normal vs 2p-2h intruder

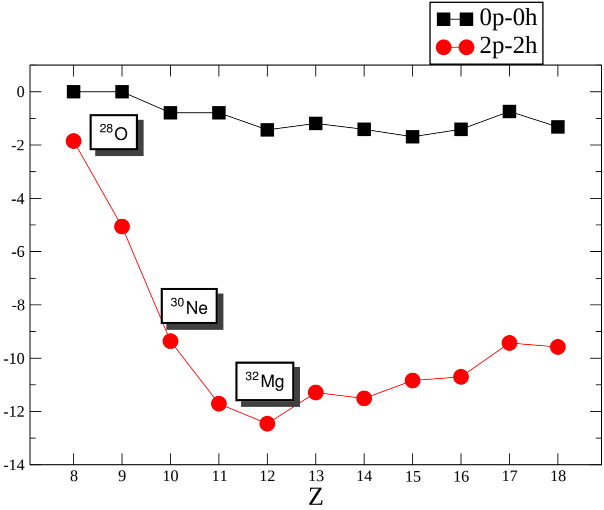

F. Nowacki and A. Poves
Phys. Rev. **C90**, 014302 (2014)

Correlations energies: normal vs 2p-2h intruder

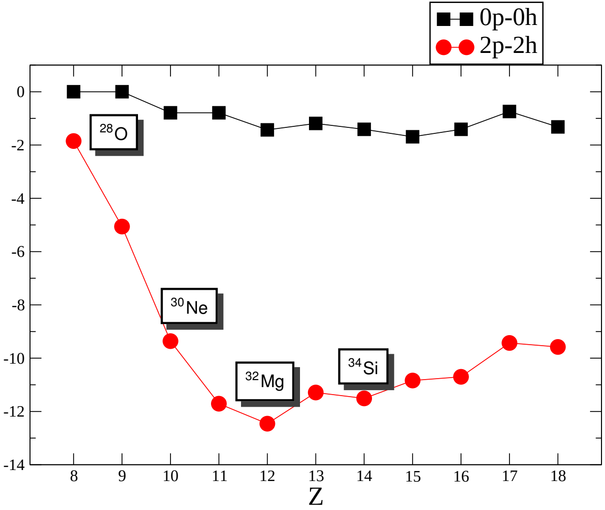

F. Nowacki and A. Poves
Phys. Rev. **C90**, 014302 (2014)

Gaps: normal vs 2p-2h intruder

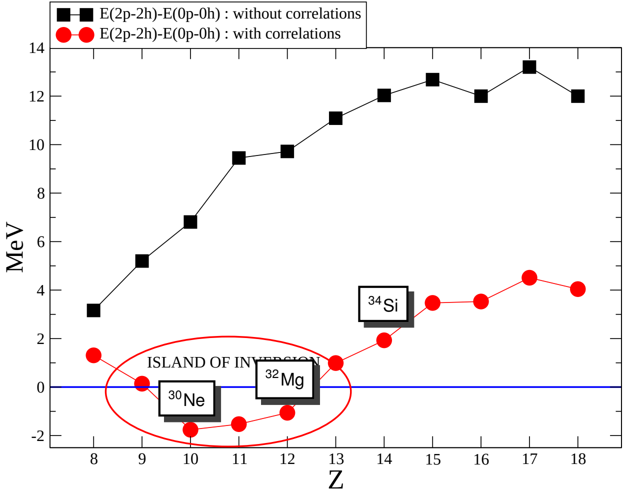

F. Nowacki and A. Poves
Phys. Rev. **C90**, 014302 (2014)

Merging of the islands of inversion at N=20 and N=28

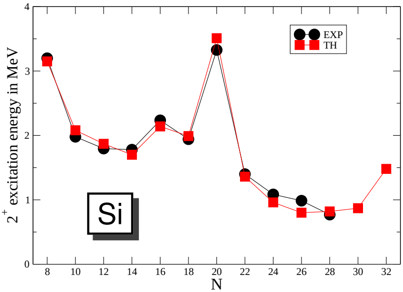

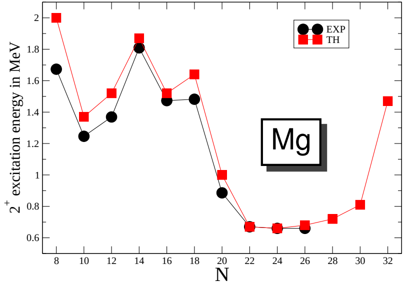

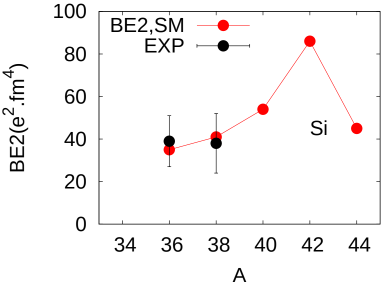

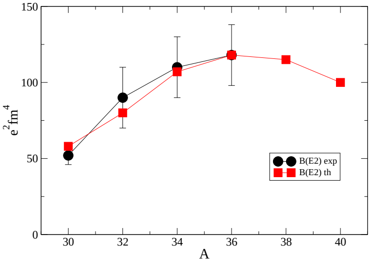

Merging of the islands of inversion at N=20 and N=28

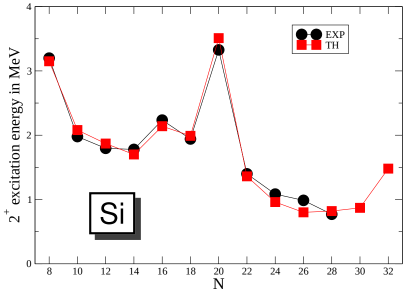

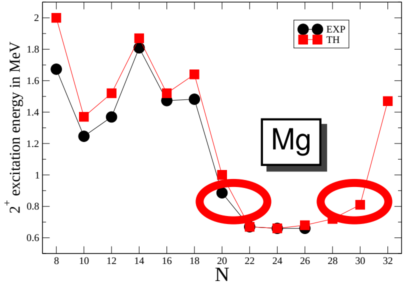

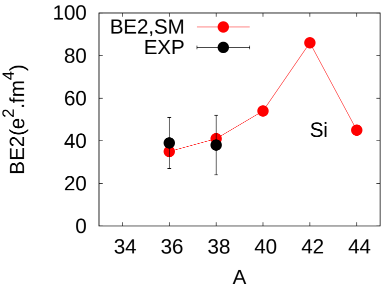

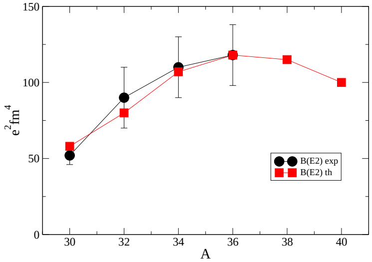

Merging of the islands of inversion at N=20 and N=28

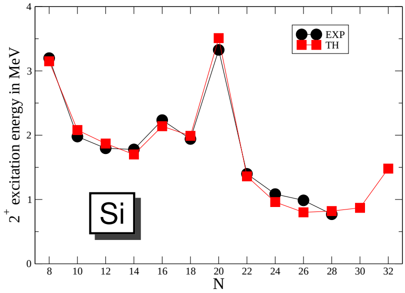

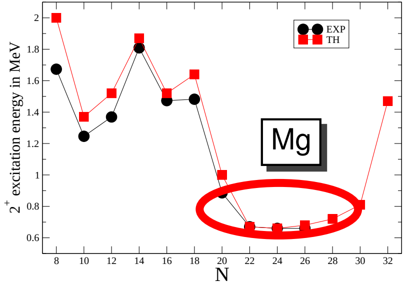

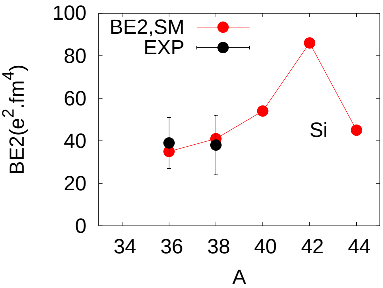

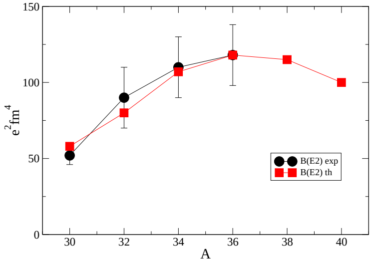

Merging of the islands of inversion at N=20 and N=28

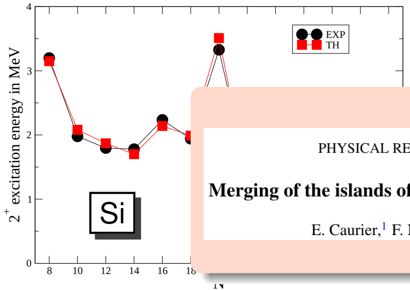

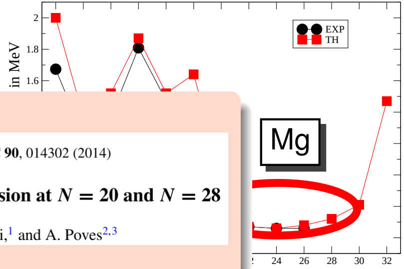

PHYSICAL REVIEW C **90**, 014302 (2014)

Merging of the islands of inversion at $N = 20$ and $N = 28$

E. Caurier,[1] F. Nowacki,[1] and A. Poves[2,3]

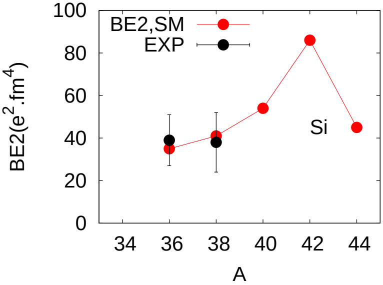

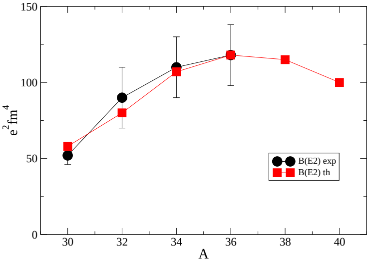

Island of inversion at N=40, an old story: 1996

ER and FE AROUND N=40

A NEW REGION OF DEFORMATION.

A. Poves

^{64}Cr

$$g(0ph-2ph) = 5.70$$
$$g(0ph-4ph) = 8.30$$

$$Q = -9.0\ b^2$$
$$BE2 = 19.8\ b^4$$

$$CS < 1\%$$
$$n(d_{5/2}) = 1.1$$

$$\frac{E(4^+)}{E(2^+)} = 2.7$$

$$\left[\frac{E(4^+)}{E(2^+)} = (3.2)\,(3.4)\right]$$

in the intruder configurations.

A SITUATION THAT REMINDS WHAT IS KNOWN AT N=20 FFS.

Island of inversion at N=40, an old story: 2003

Eur. Phys. J. A **16**, 55–61 (2003)
DOI 10.1140/epja/i2002-10069-9

THE EUROPEAN PHYSICAL JOURNAL A

GANIL

New region of deformation in the neutron-rich $^{60}_{24}Cr_{36}$ and $^{62}_{24}Cr_{38}$

O. Sorlin[1,a], C. Donzaud[1], F. Nowacki[2], J.C. Angélique[3], F. Azaiez[1], C. Bourgeois[1], V. Chiste[1], Z. Dlouhy[4], S. Grévy[3], D. Guillemaud-Mueller[1], F. Ibrahim[1], K.-L Kratz[5], M. Lewitowicz[6], S.M. Lukyanov[7], J. Mrasek[4], Yu.-E. Penionzhkevich[7], F. de Oliveira Santos[6], B. Pfeiffer[5], F. Pougheon[1], A. Poves[8], M.G. Saint-Laurent[6], and M. Stanoiu[6]

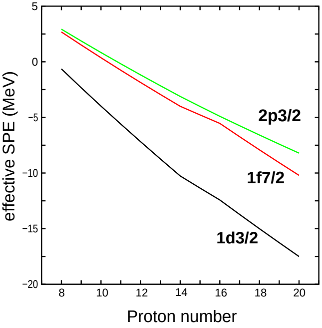

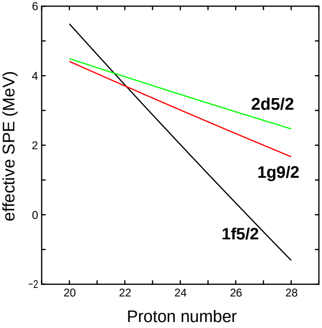

More recent experimental information

MSU

RAPID COMMUNICATIONS

PHYSICAL REVIEW C **81**, 051304(R) (2010)

Collectivity at $N = 40$ in neutron-rich ^{64}Cr

A. Gade,[1,2] R. V. F. Janssens,[3] T. Baugher,[1,2] D. Bazin,[1] B. A. Brown,[1,2] M. P. Carpenter,[3] C. J. Chiara,[3,4] A. N. Deacon,[5] S. J. Freeman,[5] G. F. Grinyer,[1] C. R. Hoffman,[3] B. P. Kay,[3] F. G. Kondev,[6] T. Lauritsen,[3] S. McDaniel,[1,2] K. Meierbachtol,[1,7] A. Ratkiewicz,[1,2] S. R. Stroberg,[1,2] K. A. Walsh,[1,2] D. Weisshaar,[1] R. Winkler,[1] and S. Zhu[3]

[1]*National Superconducting Cyclotron Laboratory, Michigan State University, East Lansing, Michigan 48824, USA*

[2]*Department of Physics and Astronomy, Michigan State University, East Lansing, Michigan 48824, USA*

[3]*Physics Division, Argonne National Laboratory, Argonne, Illinois 60439, USA*

GANIL

RAPID COMMUNICATIONS

PHYSICAL REVIEW C **81**, 061301(R) (2010)

Onset of collectivity in neutron-rich Fe isotopes: Toward a new island of inversion?

J. Ljungvall,[1,2,3] A. Görgen,[1] A. Obertelli,[1] W. Korten,[1] E. Clément,[2] G. de France,[2] A. Bürger,[4] J.-P. Delaroche,[5] A. Dewald,[6] A. Gadea,[7] L. Gaudefroy,[5] M. Girod,[5] M. Hackstein,[6] J. Libert,[8] D. Mengoni,[9] F. Nowacki,[10] T. Pissulla,[6] A. Poves,[11] F. Recchia,[12] M. Rejmund,[2] W. Rother,[6] E. Sahin,[12] C. Schmitt,[2] A. Shrivastava,[2] K. Sieja,[10] J. J. Valiente-Dobón,[12] K. O. Zell,[6] and M. Zielińska[13]

[1]*CEA Saclay, IRFU, Service de Physique Nucléaire, F-91191 Gif-sur-Yvette, France*

[2]*GANIL, CEA/DSM-CNRS/IN2P3, Bd Henri Becquerel, BP 55027, F-14076 Caen, France*

SM framework

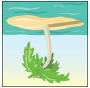

Island of inversion around ^{64}Cr

S. Lenzi, F. Nowacki, A. Poves and K. Sieja

Phys. Rev. C 82, 054301, 2010.

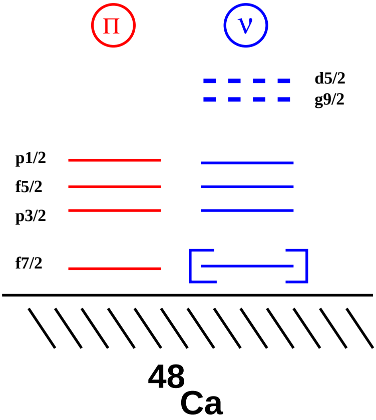

LNPS interaction:

- based on realistic TBME
- new fit of the pf shell (KB3GR, E. Caurier)
- monopole corrections
- $g_{9/2}$-$d_{5/2}$ gap set to 1.5 Mev in ^{68}Ni

Calculations:

- up to 14p-14h excitations across Z=28 and N=40 gaps
- up to 10^{10}
- m-scheme code ANTOINE (non public version)

Shape transition at N=40

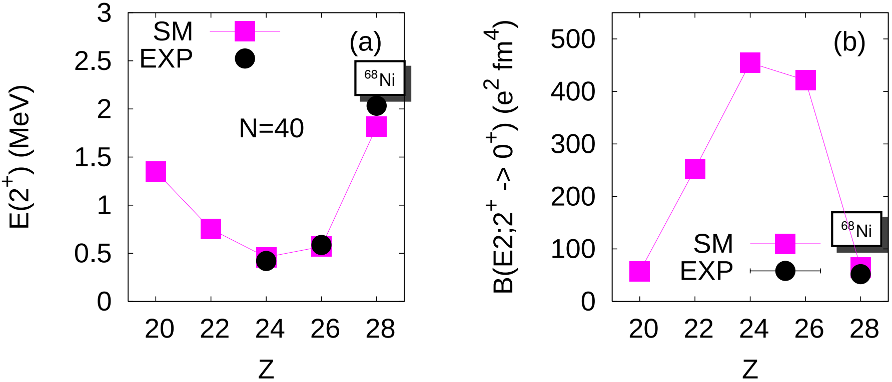

Nucleus	$\nu g_{9/2}$	$\nu d_{5/2}$	configuration
^{68}Ni	0.98	0.10	0p0h(51%)
^{66}Fe	3.17	0.46	4p4h(26%)
^{64}Cr	3.41	0.76	6p6h(23%)
^{62}Ti	3.17	1.09	4p4h(48%)

Shape transition at N=40

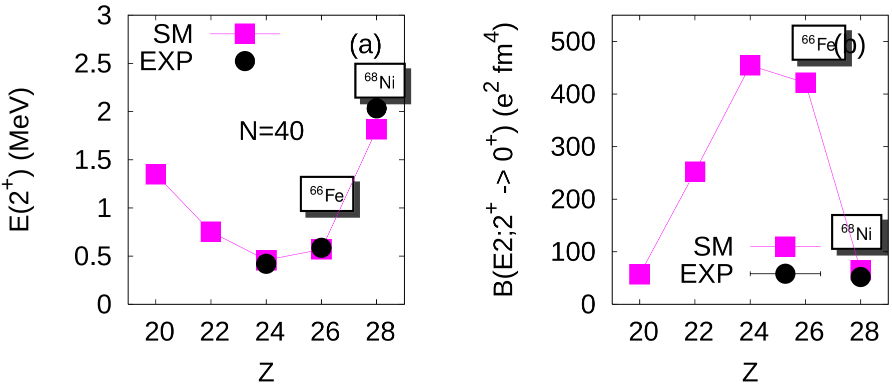

Nucleus	$\nu g_{9/2}$	$\nu d_{5/2}$	configuration
^{68}Ni	0.98	0.10	0p0h(51%)
^{66}Fe	3.17	0.46	4p4h(26%)
^{64}Cr	3.41	0.76	6p6h(23%)
^{62}Ti	3.17	1.09	4p4h(48%)

Shape transition at N=40

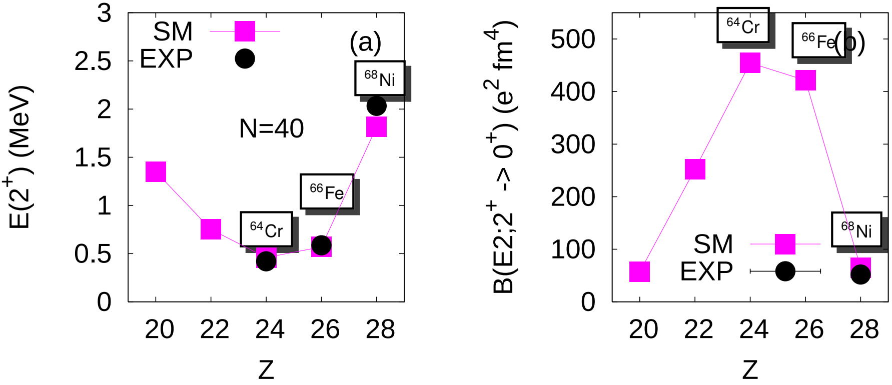

Nucleus	$\nu g_{9/2}$	$\nu d_{5/2}$	configuration
^{68}Ni	0.98	0.10	0p0h(51%)
^{66}Fe	3.17	0.46	4p4h(26%)
^{64}Cr	3.41	0.76	6p6h(23%)
^{62}Ti	3.17	1.09	4p4h(48%)

Neutron effective single particle energies

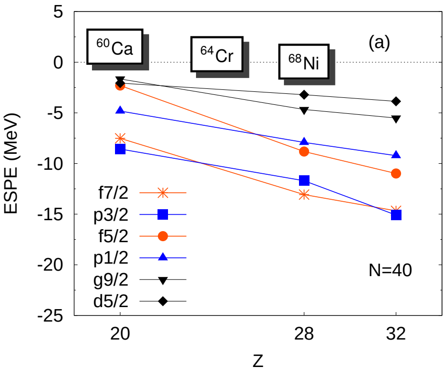

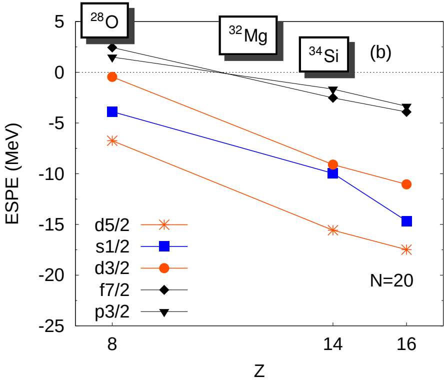

- reduction of the $\nu f_{5/2}$-$g_{9/2}$ gap with removing $f_{7/2}$ protons
- proximity of the quasi-SU3 partner $d_{5/2}$
- inversion of $d_{5/2}$ and $g_{9/2}$ orbitals
  same ordering as CC calculations

- reduction of the $\nu d_{3/2}$-$f_{7/2}$ gap with removing $d_{5/2}$ protons
- proximity of the quasi-SU3 partner $p_{3/2}$
- inversion of $p_{3/2}$ and $f_{7/2}$ orbitals

Neutron effective single particle energies

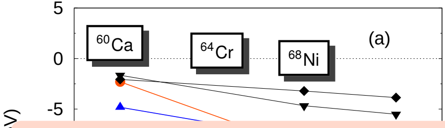

PRL **109,** 032502 (2012) PHYSICAL RE

TABLE II. Energies of the $5/2^+$ and $9/2^+$ resonances in ^{53,55,61}Ca. Re[E] is the energy relative to the one-neutron emission threshold, and the width is $\Gamma = -2\text{Im}[E]$ (in MeV).

	^{53}Ca		^{55}Ca		^{61}Ca	
J^π	Re[E]	Γ	Re[E]	Γ	Re[E]	Γ
$5/2^+$	1.99	1.97	1.63	1.33	1.14	0.62
$9/2^+$	4.75	0.28	4.43	0.23	2.19	0.02

G. Hagen et al.

Phys. Rev. Lett. **109**, 032502 (2012)

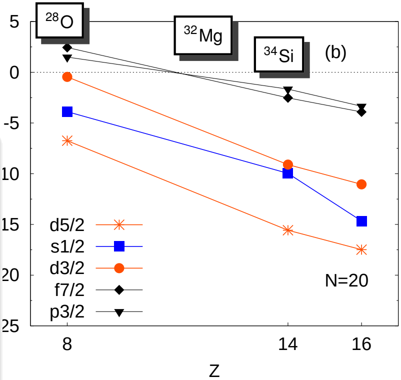

removing $f_{7/2}$ protons

- proximity of the quasi-SU3 partner $d_{5/2}$
- inversion of $d_{5/2}$ and $g_{9/2}$ orbitals
same ordering as CC calculations

- reduction of the $\nu d_{3/2}$-$f_{7/2}$ gap with removing $d_{5/2}$ protons
- proximity of the quasi-SU3 partner $p_{3/2}$
- inversion of $p_{3/2}$ and $f_{7/2}$ orbitals

Extension of collectivity N=40 towards N=50

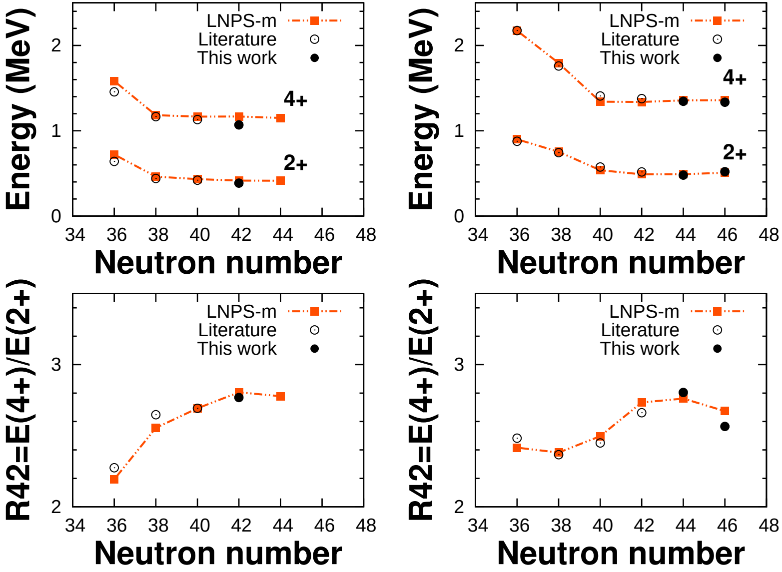

Extension of collectivity N=40 towards N=50

TABLE I: Quadrupole deformation properties of Cr and Fe isotopes. Energies are in MeV, $B(E2)$ in e^2 fm^4, and Q in e fm^2. Experimental energies are the same as Fig. 3.

	^{62}Cr	^{64}Cr	^{66}Cr	^{68}Cr	^{66}Fe	^{68}Fe	^{70}Fe	^{72}Fe
$E^*(2_1^+)$ exp.	0.44	0.42	0.39	-	0.57	0.52	0.48	0.52
$E^*(2_1^+)$ theo.	0.46	0.43	0.42	0.41	0.54	0.49	0.49	0.51
Q_{spec}	-38	-38	-39	-38	-37	-40	-39	-33
$B(E2)\downarrow$ th.	378	388	389	367	372	400	382	279
Q_{int} from Q_{spec}	135	136	137	132	131	140	135	116
Q_{int} from B(E2)	138	140	140	136	137	142	139	118
$< \beta >$	0.33	0.33	0.32	0.30	0.29	0.30	0.28	0.24
$E^*(4_1^+)$ exp.	1.17	1.13	1.07	-	1.41	1.39	1.35	1.33
$E^*(4_1^+)$ theo.	1.18	1.13	1.06	1.15	1.34	1.34	1.36	1.36
Q_{spec}	-49	-49	-46	-47	-47	-51	-48	-40
$B(E2)\downarrow$ th.	562	534	562	530	553	608	574	377
Q_{int} from Q_{spec}	135	134	134	130	129	141	132	111
Q_{int} from B(E2)	141	140	141	137	139	146	142	115
$< \beta >$	0.34	0.33	0.32	0.31	0.29	0.30	0.29	0.23

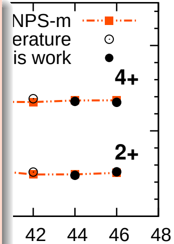

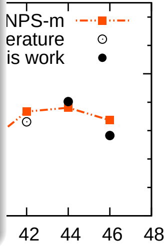

Energy (MeV)

R42=E(4+)/E(2+)

Neutron number

Neutron number

Extension of collectivity N=40 towards N=50

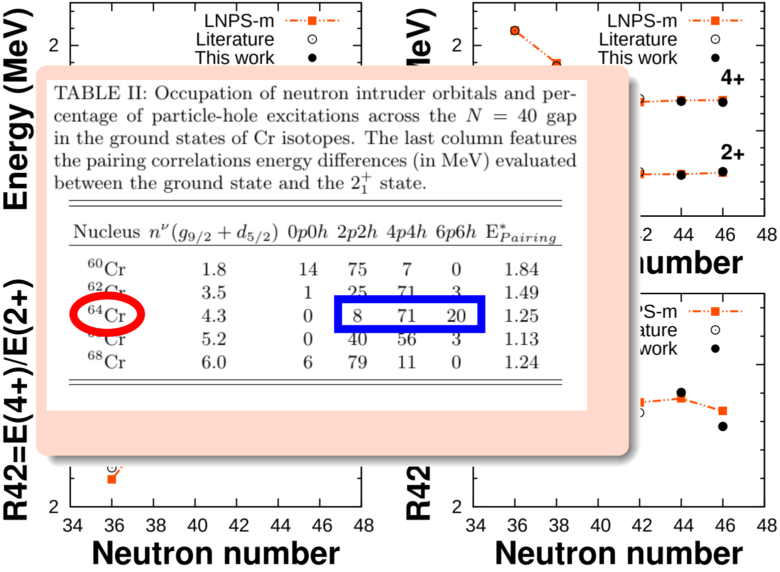

TABLE II: Occupation of neutron intruder orbitals and percentage of particle-hole excitations across the $N = 40$ gap in the ground states of Cr isotopes. The last column features the pairing correlations energy differences (in MeV) evaluated between the ground state and the 2_1^+ state.

Nucleus	$n^\nu(g_{9/2} + d_{5/2})$	0p0h	2p2h	4p4h	6p6h	$E^*_{Pairing}$
^{60}Cr	1.8	14	75	7	0	1.84
^{62}Cr	3.5	1	25	71	3	1.49
^{64}Cr	4.3	0	8	71	20	1.25
Cr	5.2	0	40	56	3	1.13
^{68}Cr	6.0	6	79	11	0	1.24

Extension of collectivity N=40 towards N=50

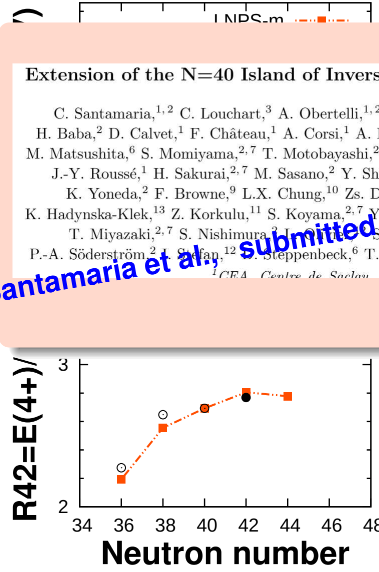

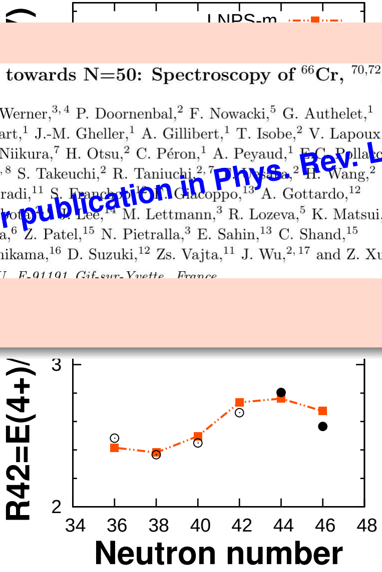

Extension of the N=40 Island of Inversion towards N=50: Spectroscopy of ^{66}Cr, ^{70,72}Fe

C. Santamaria,[1,2] C. Louchart,[3] A. Obertelli,[1,2] V. Werner,[3,4] P. Doornenbal,[2] F. Nowacki,[5] G. Authelet,[1] H. Baba,[2] D. Calvet,[1] F. Château,[1] A. Corsi,[1] A. Delbart,[1] J.-M. Gheller,[1] A. Gillibert,[1] T. Isobe,[2] V. Lapoux,[1] M. Matsushita,[6] S. Momiyama,[2,7] T. Motobayashi,[2] M. Niikura,[7] H. Otsu,[2] C. Péron,[1] A. Peyaud,[1] E.C. Pollacco,[1] J.-Y. Roussé,[1] H. Sakurai,[2,7] M. Sasano,[2] Y. Shiga,[2,8] S. Takeuchi,[2] R. Taniuchi,[2,7] T. Uesaka,[2] H. Wang,[2] K. Yoneda,[2] F. Browne,[9] L.X. Chung,[10] Zs. Dombradi,[11] S. Franchoo,[12] F. Giacoppo,[13] A. Gottardo,[12] K. Hadynska-Klek,[13] Z. Korkulu,[11] S. Koyama,[2,7] Y. Kubota,[2,6] J. Lee,[14] M. Lettmann,[3] R. Lozeva,[5] K. Matsui,[2,7] T. Miyazaki,[2,7] S. Nishimura,[2] L. Olivier,[12] S. Ota,[6] Z. Patel,[15] N. Pietralla,[3] E. Sahin,[13] C. Shand,[15] P.-A. Söderström,[2] I. Stefan,[12] D. Steppenbeck,[6] T. Sumikama,[16] D. Suzuki,[12] Zs. Vajta,[11] J. Wu,[2,17] and Z. Xu[14]

[1]CEA, Centre de Saclay, IRFU, F-91191 Gif-sur-Yvette, France

C. Santamaria et al., submitted for publication in Phys. Rev. Lett.

Spin-orbit shell closure far from stability

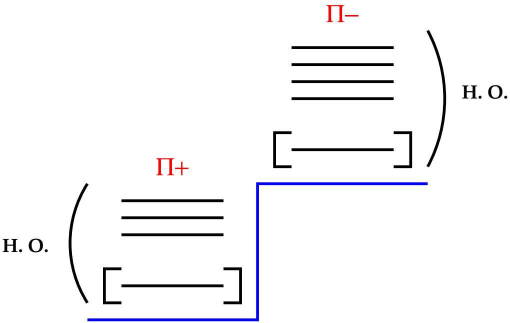

- sd-pf: ^{42}Si deformed
- pf-sdg: ^{78}Ni ???
- sdg-phf: ^{132}Sn doubly magic

- Evolution of Z=28 from N=40 to N=50
- Evolution of N=50 from Z=40 to Z=28

Three-body forces in medium mass nuclei

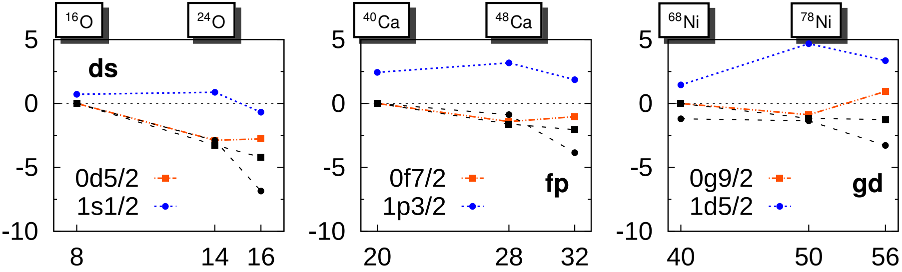

- Evolution of the neutron effective single-particle energies with neutron filling in ds, fp, and gd shells
- "Universal" mechanism for the generation of T=1 spin-orbit shell closures
- Connection with 3N forces and ab-initio calculations:
  - "works" for Coupled-Cluster and to be checked in nickels
  - problems for "ab-initio" core shell-model

Three body forces and persistence of spin-orbit shell gaps in medium-mass nuclei: Towards the doubly magic ^{78}Ni
K. Sieja, F. Nowacki
Phys. Rev. **C85**, 051301(R) (2012)

Physics around ^{78}Ni

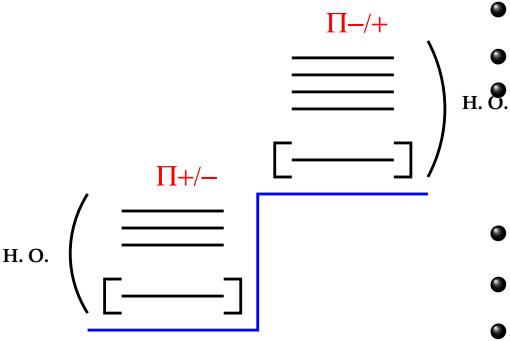

PFSDG-U interaction:

- based on realistic TBME
- pf shell for protons and gds shell for neutrons
- monopole corrections
- proton and neutrons gap ^{78}Ni fixed to phenomenological derived values

Calculations:

- excitations across Z=28 and N=50 gaps
- up to 10^{10} Slater Determinant basis states
- m-scheme code ANTOINE (non public version)

Physics around ^{78}Ni

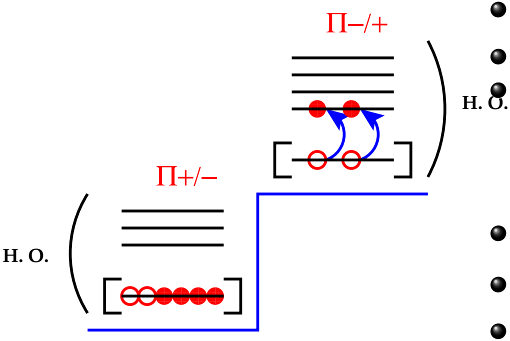

PFSDG-U interaction:

- based on realistic TBME
- pf shell for protons and gds shell for neutrons
- monopole corrections
- proton and neutrons gap ^{78}Ni fixed to phenomenological derived values

Calculations:

- excitations across Z=28 and N=50 gaps
- up to 10^{10} Slater Determinant basis states
- m-scheme code ANTOINE (non public version)

Island of Deformation below ^{78}Ni

Schematic SU3 predictions: arXiv 1404.0224

Nilsson-SU3 selfconsistency:
Quadrupole dominance in heavy N=Z nuclei

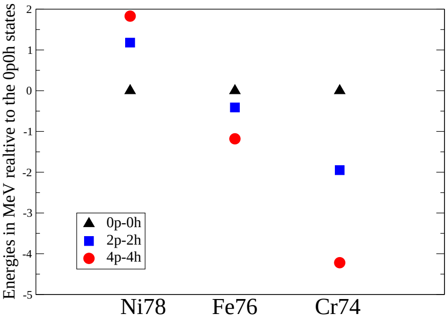

- monopole + quadrupole model
- proton gap (5MeV) and neutron gap (5 MeV) estimates
- Quasi-SU3 (protons) and Pseudo-SU3 (neutrons) blocks
- $Q_s = (\langle 2q_{20} \rangle + 3.)b^2)^2/3.5$

  $$E = \epsilon_i \langle n_i \rangle - \hbar\omega\kappa(\frac{\langle 2q_{20(3)} \rangle}{15} + \frac{\langle 2q_{20(4)} \rangle}{23})$$
- Prediction of Island of strong collectivity below ^{78}Ni !!!

Shape coexistence in ^{78}Ni

- At first approximation, ^{78}Ni has a double closed shell structure for GS
- But very low-lying 4*p*4*h* structures
- The first excited state 2_1^+ in ^{78}Ni predicted at 2.8 MeV and to be a deformed intruder !!!
- Necessity to go beyond $(fpg_{\frac{9}{2}} d_{\frac{5}{2}})$ LNPS space

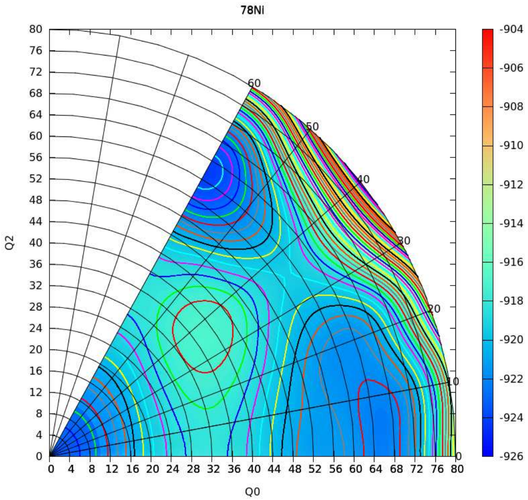

Constrained deformed HF in the SM basis

(B. Bounthong, Ph D Thesis, Strasbourg)

Island of Deformation below ^{78}Ni

Schematic SU3 predictions: arXiv 1404.0224

Nilsson-SU3 selfconsistency:
Quadrupole dominance in heavy N=Z nuclei

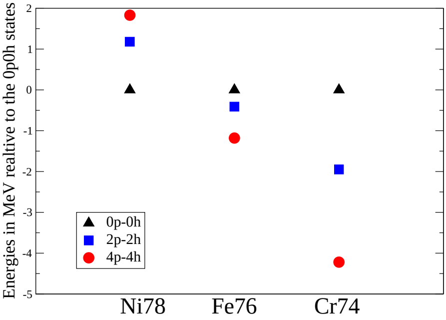

- monopole + quadrupole model
- proton gap (5MeV) and neutron gap (5 MeV) estimates
- Quasi-SU3 (protons) and Pseudo-SU3 (neutrons) estimates
- $Q_s = (\langle 2q_{20} \rangle + 3.)b^2)^2/3.5$

$$E = \epsilon_i \langle n_i \rangle - \hbar\omega\kappa(\frac{\langle 2q_{20(3)} \rangle}{15} + \frac{\langle 2q_{20(4)} \rangle}{23})$$

- Prediction of Island of strong collectivity below ^{78}Ni !!!

Island of Deformation below ^{78}Ni

Schematic SU3 predictions: arXiv 1404.0224

Nilsson-SU3 selfconsistency:
Quadrupole dominance in heavy N=Z nuclei

	$E^*(2_1^+)$ (MeV)	Q_s (e.fm^2)	BE2↓ (e^2.fm^4)	Q_i from Q_s	Q_i from from BE2	β
^{72}Cr	0.24	-48	551	167	166	0.37
^{74}Cr	0.29	-46	515	162	161	0.36
^{76}Cr	0.41	-29	239	100	108	0.22
^{76}Fe	0.35	-39	346	135	132	0.26

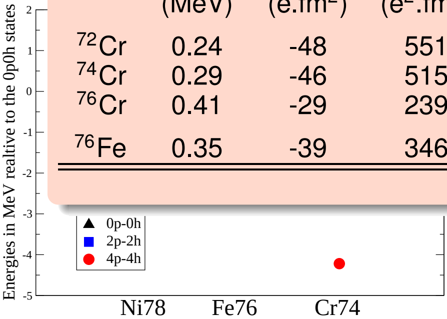

$E = \epsilon_i \langle n_i \rangle - \hbar\omega\kappa(\frac{[illegible]}{15} + \frac{[illegible]}{23})$

- Prediction of Island of strong collectivity below ^{78}Ni !!!

Schematic SU3 predictions: arXiv 1404.0224

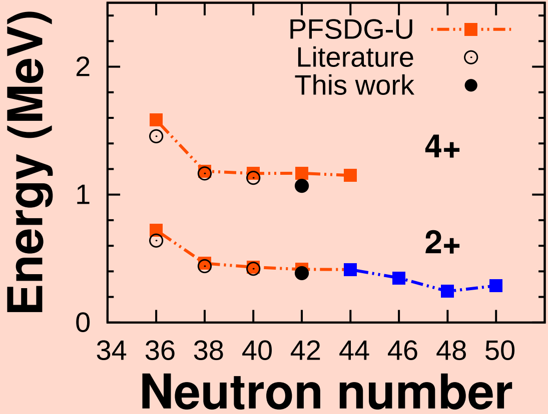

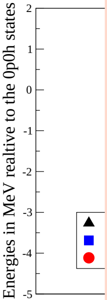

Extension of Island of deformation to N=50 !!!

gap (5

o-SU3

$\frac{20(4)\rangle}{23}$)

lectivity

Spin-orbit shell closure far from stability

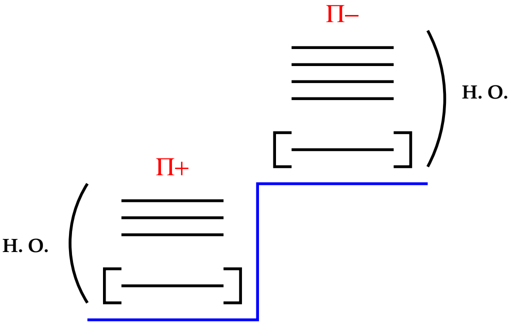

- sd-pf: ^{42}Si deformed
- pf-sdg: ^{78}Ni ???
- sdg-phf: ^{132}Sn doubly magic

- Evolution of Z=28 from N=40 to N=50
- Evolution of N=50 from Z=40 to Z=28

Effective Single Particle Energies: Trends

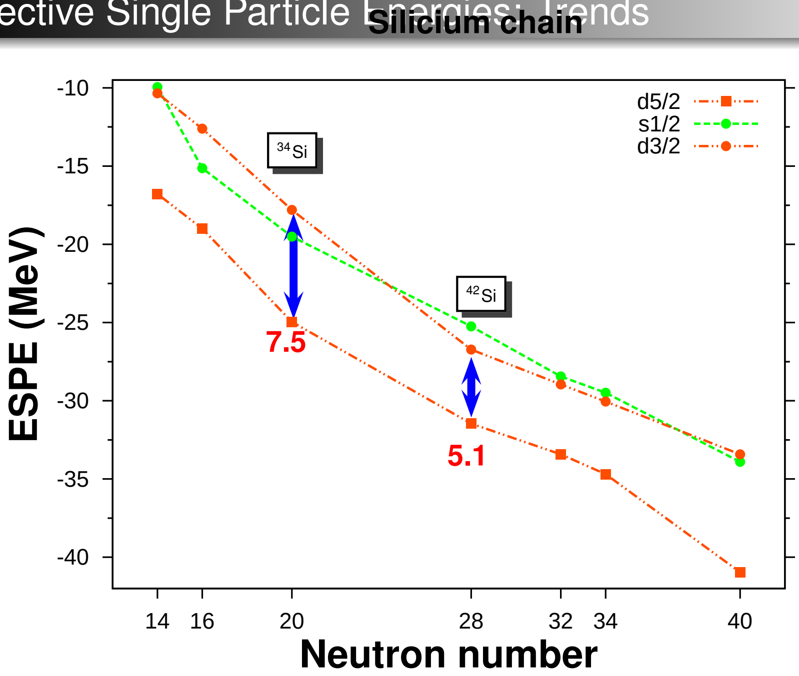

Effective Single Particle Energies: Trends

Silicium chain

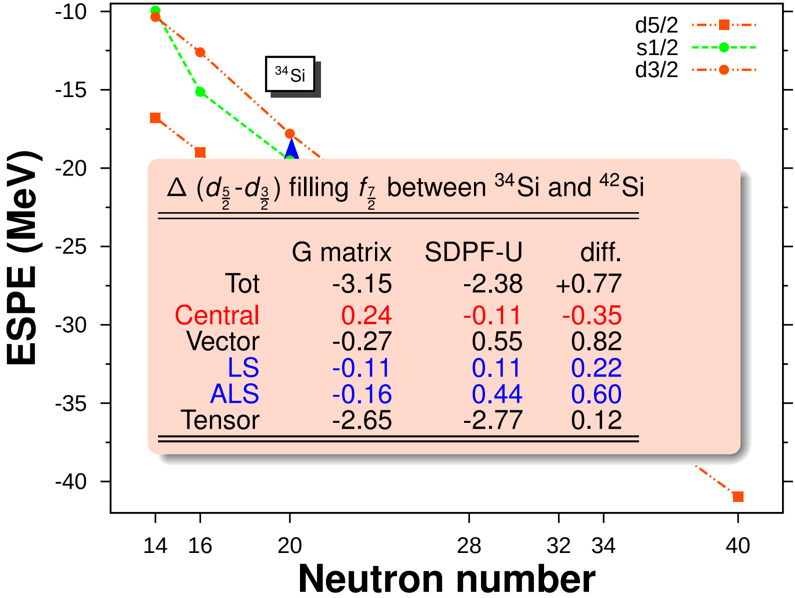

$\Delta\ (d_{\frac{5}{2}}\text{-}d_{\frac{3}{2}})$ filling $f_{\frac{7}{2}}$ between ^{34}Si and ^{42}Si

	G matrix	SDPF-U	diff.
Tot	-3.15	-2.38	+0.77
Central	0.24	-0.11	-0.35
Vector	-0.27	0.55	0.82
LS	-0.11	0.11	0.22
ALS	-0.16	0.44	0.60
Tensor	-2.65	-2.77	0.12

Silicium chain

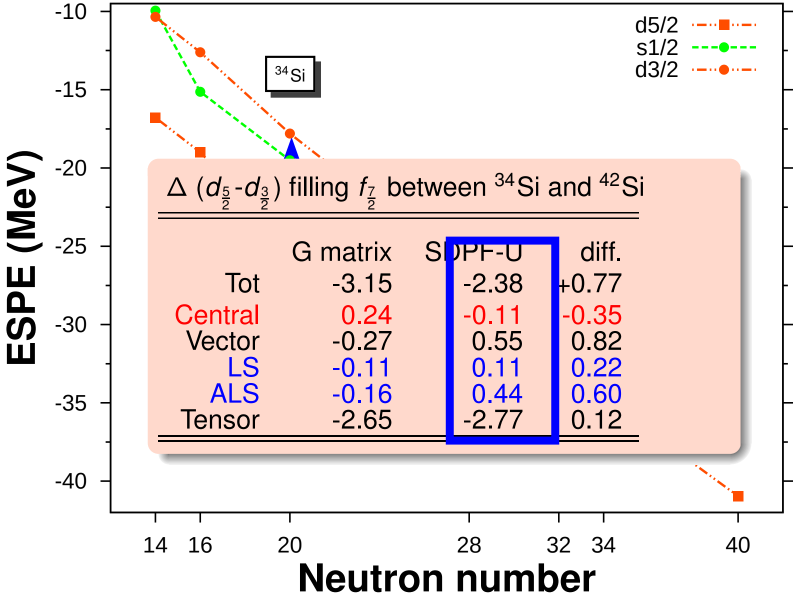

Δ ($d_{\frac{5}{2}}$-$d_{\frac{3}{2}}$) filling $f_{\frac{7}{2}}$ between ^{34}Si and ^{42}Si

	G matrix	SDPF-U	diff.
Tot	-3.15	-2.38	+0.77
Central	0.24	-0.11	-0.35
Vector	-0.27	0.55	0.82
LS	-0.11	0.11	0.22
ALS	-0.16	0.44	0.60
Tensor	-2.65	-2.77	0.12

Effective Single Particle Energies: Trends

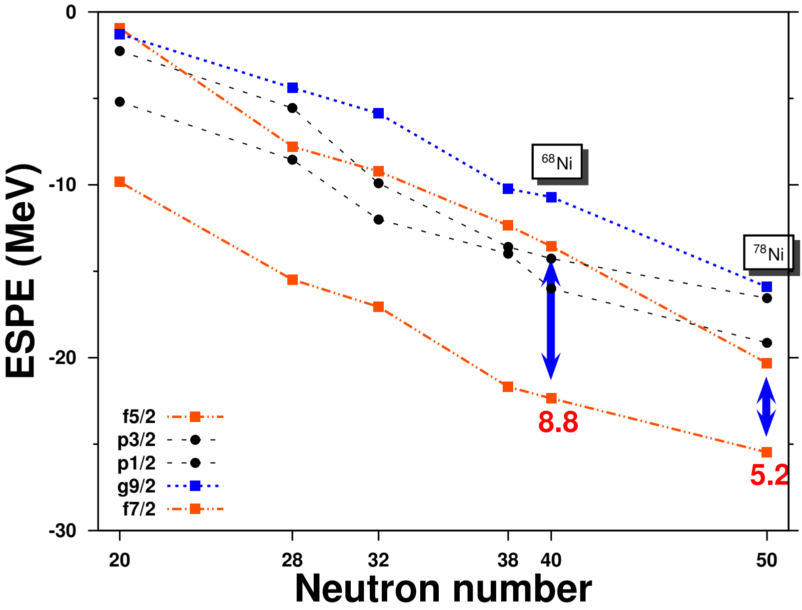

Effective Single Particle Energies: Trends

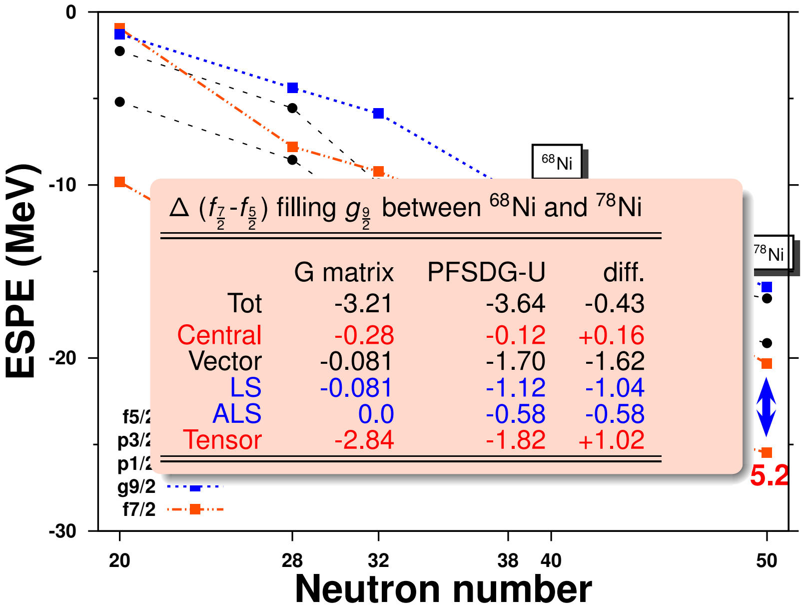

Δ ($f_{\frac{7}{2}}$-$f_{\frac{5}{2}}$) filling $g_{\frac{9}{2}}$ between ^{68}Ni and ^{78}Ni

	G matrix	PFSDG-U	diff.
Tot	-3.21	-3.64	-0.43
Central	-0.28	-0.12	+0.16
Vector	-0.081	-1.70	-1.62
LS	-0.081	-1.12	-1.04
ALS	0.0	-0.58	-0.58
Tensor	-2.84	-1.82	+1.02

Effective Single Particle Energies: Trends

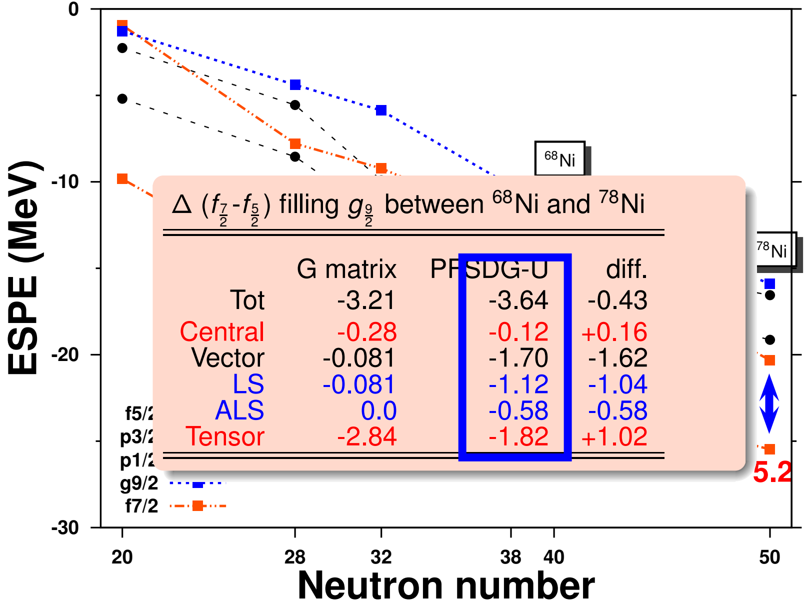

$\Delta\ (f_{\frac{7}{2}} - f_{\frac{5}{2}})$ filling $g_{\frac{9}{2}}$ between ^{68}Ni and ^{78}Ni

	G matrix	PFSDG-U	diff.
Tot	-3.21	-3.64	-0.43
Central	-0.28	-0.12	+0.16
Vector	-0.081	-1.70	-1.62
LS	-0.081	-1.12	-1.04
ALS	0.0	-0.58	-0.58
Tensor	-2.84	-1.82	+1.02

Effective Single Particle Energies: Trends

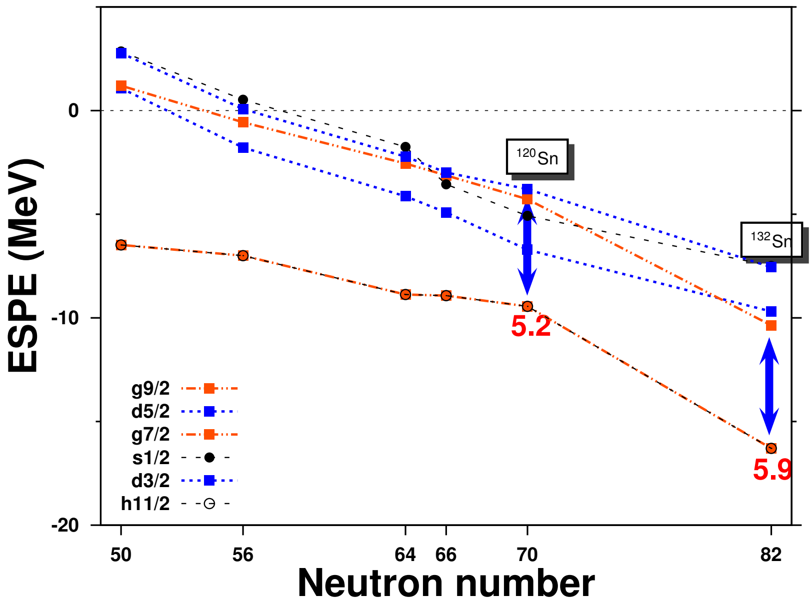

Effective Single Particle Energies: Trends

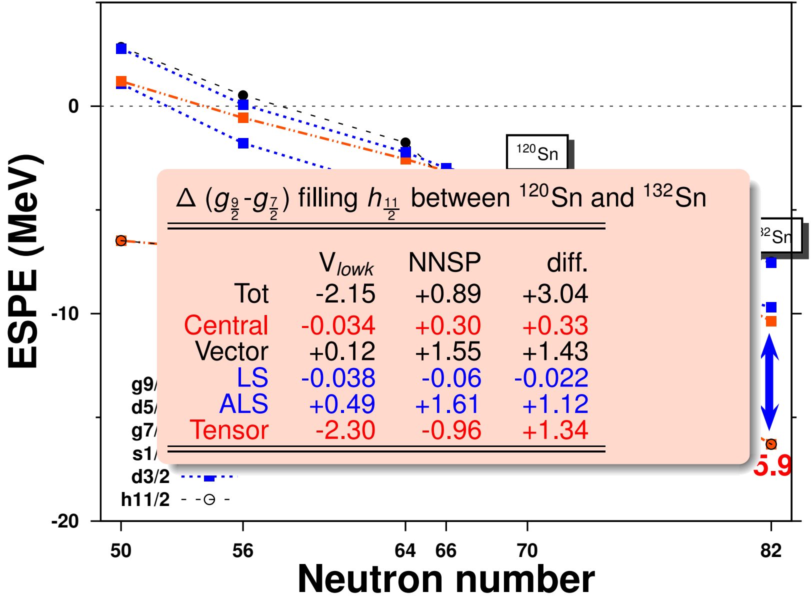

$\Delta\ (g_{\frac{9}{2}} - g_{\frac{7}{2}})$ filling $h_{\frac{11}{2}}$ between ^{120}Sn and ^{132}Sn

	V_{lowk}	NNSP	diff.
Tot	-2.15	+0.89	+3.04
Central	-0.034	+0.30	+0.33
Vector	+0.12	+1.55	+1.43
LS	-0.038	-0.06	-0.022
ALS	+0.49	+1.61	+1.12
Tensor	-2.30	-0.96	+1.34

Effective Single Particle Energies: Trends

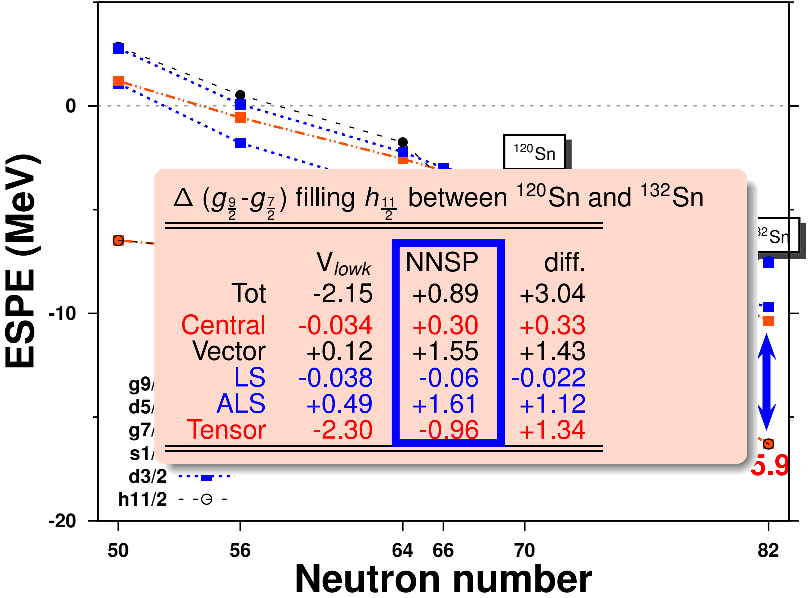

Δ $(g_{\frac{9}{2}}$-$g_{\frac{7}{2}})$ filling $h_{\frac{11}{2}}$ between ^{120}Sn and ^{132}Sn

	V_{lowk}	NNSP	diff.
Tot	-2.15	+0.89	+3.04
Central	-0.034	+0.30	+0.33
Vector	+0.12	+1.55	+1.43
LS	-0.038	-0.06	-0.022
ALS	+0.49	+1.61	+1.12
Tensor	-2.30	-0.96	+1.34

Summary

- Monopole drift develops in all regions but the Interplay between correlations (pairing + quadrupole) and spherical mean-field (monopole field) determines the physics.
  It can vary from :
  - island of inversion at N=20 and N=40
  - deformation at Z=14, N=28 for ^{42}Si and shell weakening at Z=28, N=50 for ^{78}Ni
  - deformation extending from N=40 to N=50 for Z=24-26 for ^{74}Cr and ^{76}Fe
- The “islands of inversion” appear due to the effect of the correlations, hence they could also be called “islands of enhanced collectivity”. As quadrupole correlations are dominant in this region, most of thei inhabitants are deformed rotors. Shape transitions and coexistence show up everywhere
- Quadrupole energies can be huge and understood in terms of symmetries
- Spin-Tensor Analysis show competing trends but varying significantly from light to middle mass nuclei

Summary

Special Thanks to:

- B. Bounthong, E. Caurier, H. Naidja, K. Sieja, A. Zuker
- A. Poves
- M. Hjorth-Jensen
- H. Grawe, S. Lenzi, O. Sorlin
- J. Herzfeld